

# EPR and ESEEM Studies on Silver Hydroxymethyl Radicals in Molecular Sieves†

Jacek Michalik,<sup>a</sup> Jarosław Sadło,<sup>a</sup> Andre van der Pol<sup>b</sup> and Eduard Reijerse<sup>b</sup>

<sup>a</sup>Institute of Nuclear Chemistry and Technology, Dorodna 16, 03-195 Warsaw, Poland and <sup>b</sup>University of Nijmegen, Laboratory of Molecular Spectroscopy, 6525 ED Nijmegen, The Netherlands

Michalik J., Sadło J., van der Pol A. and Reijerse E., 1997. EPR and ESEEM Studies on Silver Hydroxymethyl Radicals in Molecular Sieves. – Acta Chem. Scand. 51: 330–333. ©Acta Chemica Scandinavica 1997.

This study focuses on silver hydroxymethyl radicals produced by  $\gamma$ -ray radiolysis of silver zeolite A and silver molecular sieves, SAPO-42, SAPO-5 and SAPO-11 loaded with methanol or ethanol. Electron paramagnetic resonance (EPR) and electron spin echo envelope modulation (ESEEM) spectroscopies have been used to study the structure and dynamics of the silver hydroxymethyl radicals stabilized in these materials. From the magnetic resonance results it was established that the EPR doublets with hfs in the range 97–180 G represent covalent  $\text{Ag}\cdot\text{CH}(\text{R})\text{OH}^+$  ( $\text{R} = \text{H}, \text{CH}_3$ ) radicals. The influence of the trapping cage size on the configuration of organosilver radicals is also discussed.

It is of great interest to immobilize organometallic catalysts on heterogeneous supports<sup>1,2</sup> because the high selectivity of many molecular catalysts can be combined with the facile product separation and catalyst recovery inherent to heterogeneous systems. Zeolite hosts might offer additional features such as diffusional or transition state selectivity. Different methods for the deposition of catalytically active organometallics onto zeolites include physisorption of neutral metal carbonyls with only weak framework interactions, diffusional blocking and ligation of transition metal cations.

We have extended the last method by utilizing radiation chemistry methods. The systems we have studied are AgNa-A zeolite and SAPO molecular sieves with intrazeolite methanol or ethanol molecules, which are adsorbed after zeolite dehydration. It has been reported earlier<sup>3</sup> that  $\gamma$ -irradiation at 77 K of the  $\text{Ag}_1\text{Na-A}/\text{CH}_3\text{OH}$  system with low silver loadings produced silver atoms and different organic radicals:  $\cdot\text{CH}_3$ ,  $\cdot\text{CHO}$  and  $\cdot\text{CH}_2\text{OH}$ . On annealing above 180 K organosilver radicals, characterized by an EPR doublet with isotropic hfs of 9.7 mT, are formed. For high silver loadings organosilver radicals appear directly after irradiation at 77 K. The silver agglomeration process in zeolites is strongly affected by the presence of methanol molecules. In dehydrated AgNa-A zeolites silver hexamers  $\text{Ag}_6^{n+}$  or trimers  $\text{Ag}_3^{2+}$  are formed on irradiation depending on initial silver content.<sup>4,5</sup> The agglomeration process also proceeds in hydrated zeolites, where the formation

of two different trimers strongly interacting with water or the zeolite framework was observed.<sup>6</sup> In the presence of methanol such clusters are not formed owing to the competition between  $\cdot\text{CH}_2\text{OH}$  radicals and  $\text{Ag}^0$  atoms for reaction with  $\text{Ag}^+$  cations.<sup>3</sup>

The main objective of this study was to elucidate the structure of organosilver radicals and their interaction with the nearby environment, to determine their stability in the zeolite matrix and their possible role as catalytic intermediates.

## Results and discussion

The EPR spectra of an  $\text{Ag}_1\text{-NaA}/\text{CH}_3\text{OH}$  sample irradiated at 77 K and annealed to 180 K are shown in Fig. 1. The isotropic doublet C with hfs 9.7 mT, which grows rapidly above 150 K represents organosilver radicals, whereas doublets B' and B with hfs 54.8 mT and 66.2 mT, respectively, were assigned to  $^{107}\text{Ag}^0$  and  $^{109}\text{Ag}^0$  atoms solvated by methanol molecules. The central triplet A represents  $\cdot\text{CH}_2\text{OH}$  radicals. The hyperfine splitting of doublet C is greatly reduced compared with the  $\text{Ag}^0$  doublets, which means that spin density is substantially delocalized beyond the silver nucleus. It was earlier postulated that organosilver radicals are formed by reaction between  $\text{Ag}^+$  ions and hydroxyalkyl radicals.<sup>3,7</sup> However, the question remains open as to whether the radical structure is  $\text{Ag}\cdot\text{OCH}_2\text{R}^+$  or  $\text{Ag}\cdot\text{CHROH}^+$ . In frozen solutions of silver perchlorate in methanol both structures have been proposed, but it is worth pointing out that the splitting of doublet C in zeolite A is distinctly

† Contribution at the 14th International Conference on Radical Ions, Uppsala, Sweden, July 1–5, 1996.

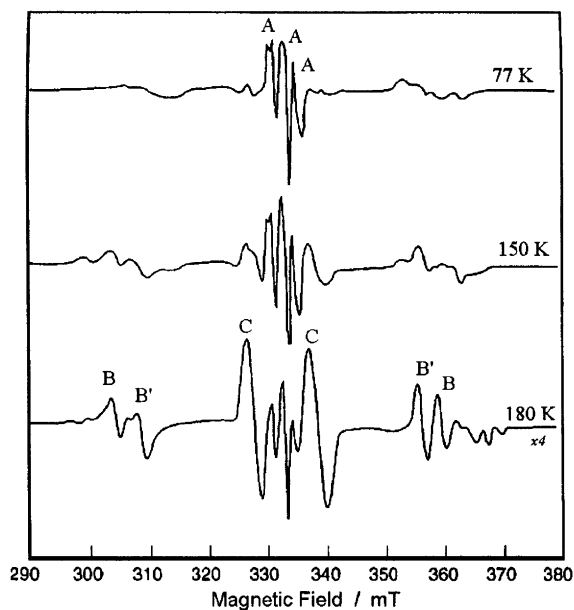


Fig. 1. The EPR spectra of an  $\text{Ag}_1\text{-NaA/CH}_3\text{OH}$  sample irradiated at 77 K and measured during thermal annealing.

smaller,  $A_{\text{iso}} = 9.7$  mT (for natural silver), than in a glassy matrix:  $A_{\text{iso}} = 13.7$  mT.

In order to prove that doublet C represents the paramagnetic species with a one-electron bond between silver and carbon,  $^{13}\text{CH}_3\text{OH}$  was adsorbed onto  $^{109}\text{Ag}_1\text{-NaA}$  zeolite. After irradiation at 77 K and annealing to 180 K the EPR spectrum clearly shows a different line pattern than for samples with  $^{12}\text{CH}_3\text{OH}$  [Fig. 2(a)]. The simulation of that spectrum, however, appeared not to be a trivial matter because of the overlap of  $^{13}\text{CH}_2\text{OH}$  and

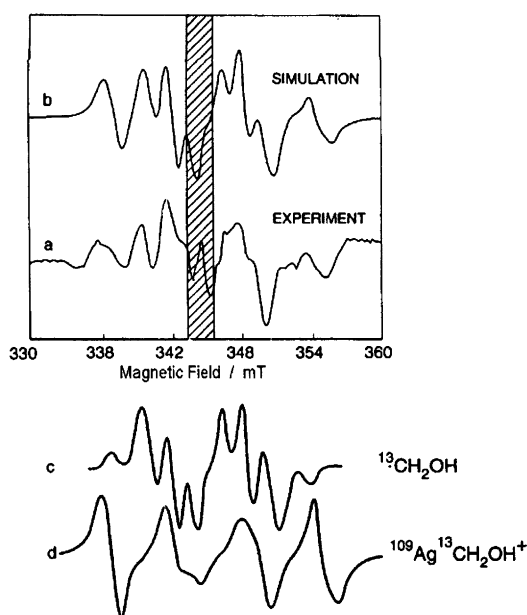


Fig. 2. Experimental and simulated EPR spectra of  $^{109}\text{Ag}_1\text{-NaA/}^{13}\text{CH}_3\text{OH}$  irradiated at 77 K and annealed to 180 K. The measurement temperature is 180 K.

$^{109}\text{Ag}^{13}\text{CH}_2\text{OH}^+$  spectra. The simulated line patterns for both radicals are shown in Fig. 2(c) and 2(d), respectively. In the simulation the anisotropic couplings of  $^{13}\text{C}$  and  $^{109}\text{Ag}$  are also taken into account. The superposition of those two spectra gives the line pattern presented in Fig. 2(b). The simulation is not perfect but can be considered to be satisfactory taking into account that irradiation also produces paramagnetic centers in the framework and Spectrosil tubings which are localized at  $g \sim 2$ . This region is shaded in Fig. 2.

It was calculated from the hyperfine splittings, obtained from the simulation, that the unpaired electron in the  $^{109}\text{Ag}^{13}\text{CH}_2\text{OH}^+$  radical is localized to the extent of 29% on Ag and 46% on C and H nuclei. By comparing these spin distributions with that in  $\cdot\text{CH}_2\text{OH}$  radical (70% on C and H) we can conclude that the  $\cdot\text{CH}_2\text{OH}$  radical shares its unpaired electron to a great extent with one  $\text{Ag}^+$  ion, resulting in  $\text{Ag}^+\cdot\text{CH}_2\text{OH}^+$ , silver hydroxymethyl radical.

To prove unequivocally the proposed structure of the silver  $\text{CH}_2\text{OH}$  adduct, pulsed EPR experiments were carried out. For two-pulse ESEEM experiments, dehydrated  $\text{AgNa-A}$  zeolite was exposed to the specifically deuteriated methanols  $\text{CH}_3\text{OD}$ ,  $\text{CD}_3\text{OH}$ ,  $\text{CD}_3\text{OD}$  and normal  $\text{CH}_3\text{OH}$ . The irradiated samples were annealed until the silver hydroxymethyl doublet reached its maximum intensity. Then two-pulse ESEEM spectra were collected setting the field on the high-field line of doublet.

The spectra presented in Fig. 3 are very different for specifically deuteriated methanol adsorbates. The recorded peaks appear at the Larmor frequencies of  $^2\text{D}$ ,  $\nu_{\text{D}}$  [Fig. 3(b),(c)] and of  $^{27}\text{Al}$ ,  $\nu_{\text{Al}}$  and at twice these

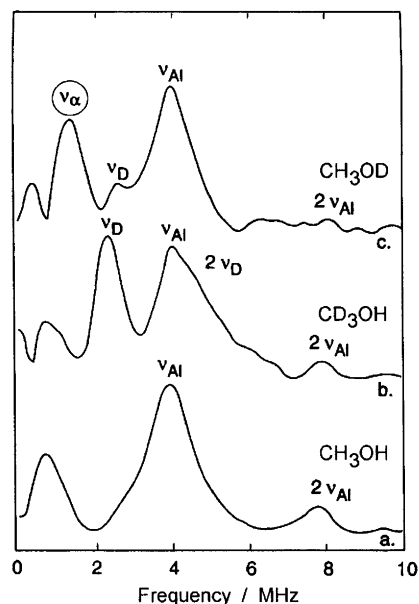


Fig. 3. Two-pulse ESEEM spectra of  $\text{Ag}_1\text{Na-A}$  zeolite exposed to the specifically deuteriated methanol molecules  $\text{CH}_3\text{OH}$  (a),  $\text{CD}_3\text{OH}$  (b),  $\text{CH}_3\text{OD}$  (c) after  $\gamma$ -ray irradiation and annealing. The magnetic field was set at the high-field line of the EPR spectra.

frequencies,  $2\nu_D$  and  $2\nu_{Al}$ . These four peaks are due to interactions of the unpaired electron with remote  $^2D$  nuclei of surrounding methanol molecules and to  $^{27}Al$  nuclei of the zeolite framework.

Comparing the spectra of  $Ag_1Na-A/CH_3OH$  and  $Ag_1Na-A/CD_3OH$  systems [Fig. 3(a) and 3(b)] it is noticeable that the only differences are the peaks due to distant molecules containing  $^2D$  nuclei [ $\nu_D$  and  $2\nu_D$  in Fig. 3(b)]. Peaks due to  $^2D$  nuclei present in  $Ag\cdot CD_2OH^+$  are not observed. This can be explained since it is known that nearby nuclei with relatively large hyperfine interactions do not give rise to an observable ESEEM pattern. The spectrum shown in Fig. 3(c) for  $Ag_1Na-A/CD_3OH$  system clearly shows a new peak, indicated as  $\nu_\alpha$ . This new peak can be due only to the  $^2D$  atom of the OD group. To explain the spectrum we have to assume that there is a second peak,  $\nu_\beta$ , coinciding with the  $^{27}Al$  peak at frequency  $\nu_{Al}$ .

To confirm the existence of this hidden peak a three-pulse experiment was carried out. Fig. 4 shows, in trace b, the experimental three-pulse spectrum in which the  $^{27}Al$  peak is suppressed. As predicted, the hidden peak shows up at about 3.8 MHz. In Fig. 4(a) a simulation is shown taking into account couplings to the  $^2D$  nucleus of the OD group and distant D nuclei of neighbouring molecules. The main features of the experimental spectrum are reproduced. The dipolar coupling parameter  $T = +1.4$  MHz obtained from the simulation corresponds to an average distance of unpaired electron to the hydroxyl  $^2D$  nucleus of 2.05 Å. For the  $\cdot CH_2OD$  radical this distance was found 1.99 Å. Apparently in  $Ag\cdot CH_2OD^+$  the average position of the electron is between the C and Ag nuclei. In all ESEEM spectra, the low frequency peak,  $\nu < 1$  MHz, is due to dead time effects.

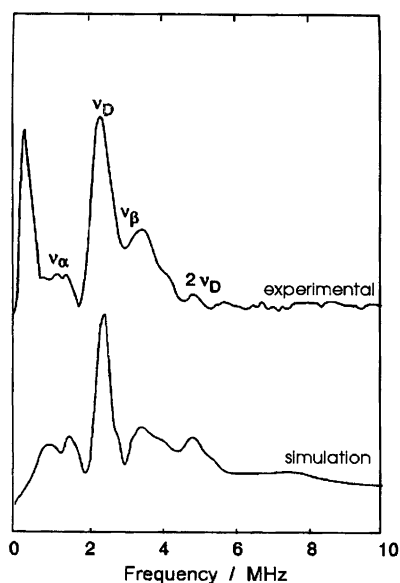


Fig. 4. Three-pulse ESEEM spectrum of  $Ag_1Na-A$  zeolite exposed to  $CH_3OD$ ,  $\gamma$ -ray irradiated and annealed. Trace b is the experimental spectrum, trace a is the simulation.

Organosilver radicals are also formed in the presence of ethanol in zeolite cages. The doublet  $C'$  assigned to the  $Ag\cdot CH(CH_3)OH^+$  radical recorded at 165 K shows some unresolved structure in the central region of the spectrum (Fig. 5). At 15 K new lines are clearly seen and the EPR spectrum can be described as a doublet of doublets with  $hfs = 10.2$  mT and 4.0 mT. Because the additional splitting at 15 K does not appear when organosilver radicals are formed in zeolite containing  $CH_3OH$  or  $C_2D_5OH$  alcohols it can be associated only with the interaction of  $\beta$ -methyl protons of the ethanol molecule. The proposed structure of the silver hydroxyethyl radical is also shown in Fig. 5. It is postulated that the methyl group in  $Ag\cdot CH(CH_3)OH^+$  radical rotates about the C-C bond above 165 K. At lower temperatures the rotation ceases and the interaction with one proton becomes predominant. If relatively rapid rotation about the C-C bond occurs, the interactions with the methyl protons is averaged out and the additional 4.0 mT splitting is not observed.

The EPR doublets of silver hydroxymethyl radicals have also been observed in other molecular sieves. The Ag hyperfine splittings of  $Ag\cdot CH_2OH^+$  for methanol glass and for different molecular sieves are listed in Table 1. The splittings are substantially different for various molecular sieves, ranging from 9.7 mT for zeolite A to 18.0 mT for SAPO-11. This means that the spin density on Ag is nearly a factor of two higher for  $Ag\cdot CH_2OH^+$  in SAPO-11. From Table 1 it seems evident that there is a correlation, at least for SAPOs, between the size of trapping cages and the hyperfine splitting. The smaller the size of cage the larger the hfs. Thus, it seems reasonable to assume that in smaller cages, because of steric hindrance, the configuration of the silver hydroxymethyl radical is distorted to some extent, which might affect spin density distribution. The observed differences in hfs values for hydroxymethyl radicals in isostructural

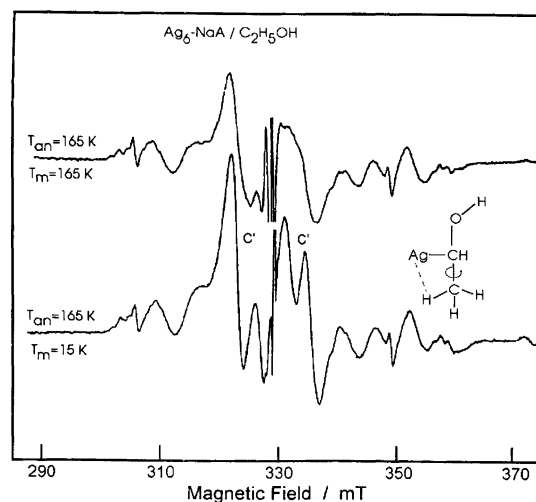


Fig. 5. The EPR spectra of an  $Ag_8-NaA/C_2H_5OH$  sample recorded at 165 K and 15 K. The sample was annealed to 165 K.

Table 1. Hyperfine splittings of the  $\text{Ag}\cdot\text{CH}_2\text{OH}^+$  radical in various matrices.

Matrix	MeOH glass	Zeolites with MeOH			
		A	SAPO-42	SAPO-11	SAPO-5
hfs/mT	13.7	9.7	13.7	18.0	15.0
Cavity size/Å	—	11.6	11.6	6.4 × 4.0	7.3 × 7.3

zeolite A and SAPO-42 can also be explained by different kinds of steric hindrance, although the  $\alpha$ -cages are the same in both structures. The total cation capacity is, however, one order of magnitude higher in zeolite A than in SAPO-42.<sup>8</sup> This makes the effective volume of the  $\alpha$ -cage in A zeolite much smaller resulting in a bigger radical distortion.

### Conclusions

Silver hydroxymethyl radicals as evidenced by EPR doublets with hfs in the range 9.7–18.0 mT are the major secondary products of radiolysis of silver molecular sieves exposed to methanol before irradiation. Based on the EPR results of  $^{109}\text{Ag}_1\text{-NaA}$  exposed to  $^{13}\text{CH}_3\text{OH}$  the formation of the  $^{109}\text{Ag}\cdot^{13}\text{CH}_2\text{OH}^+$  radical with a one-electron-bond  $\text{Ag}\cdot\text{C}$  was postulated. This hypothesis was confirmed by pulsed EPR experiments. The differences in the hfs values for  $\text{Ag}\cdot\text{CH}_2\text{OH}^+$  in various molecular sieves were assigned to distorted radical configurations caused by steric hindrance.

In molecular sieves with adsorbed ethanol, silver ethanol radicals are formed. The observed changes in the EPR spectra around 165 K were assigned to the methyl group rotation in the  $\text{Ag}\cdot\text{CH}(\text{CH}_3)\text{OH}^+$  radical.

### References

1. Lamb, H. H., Gates, B. C. and Knozinger, H. *Angew. Chem., Chem. Int. Ed. Engl.* 27 (1988) 1127.
2. Basset, J. M. and Choplin, A. *J. Mol. Catal.* 21 (1983) 95.
3. Wasowicz, T., Mikosz, J., Sadło, J. and Michalik, J. *J. Chem. Soc., Perkin Trans. 2* (1992) 1487.
4. Michalik, J. and Kevan, L. *J. Am. Chem. Soc.* 108 (1986) 4247.
5. Van der Pol, A., Reijerse, E. J., de Boer, E., Wasowicz, T. and Michalik, J. *J. Mol. Phys.* 75 (1992) 37.
6. Michalik, J., Wasowicz, T., van der Pol, A., Reijerse, E. J. and de Boer, E. *J. Chem. Soc., Chem. Commun.* (1992) 29.
7. Symons, M. C. R., Janes, R. and Stevens, A. D. *Chem. Phys. Lett.* 160 (1989) 386.
8. Michalik, J., Zamadics, M., Sadło, J. and Kevan, L. *J. Phys. Chem.* 97 (1993) 10440.

Received August 8, 1996.